

## Hyperfine transition in light muonic atoms of odd $Z$

T. J. Stocki,\* D. F. Measday, E. Gete,<sup>†</sup> M. A. Saliba,<sup>‡</sup> and J. Lange,<sup>§</sup>

*Department of Physics and Astronomy, University of British Columbia, Vancouver, British Columbia, Canada V6T 1Z1*

T. P. Gorringer

*Department of Physics and Astronomy, University of Kentucky, Lexington, Kentucky 40506-0055*

(Received 7 February 2001; published 13 September 2001)

The hyperfine (hf) transition rates for muonic atoms have been remeasured for select light nuclei, using neutron detectors to evaluate the time dependence of muon capture. For  $^{19}\text{F}$   $\Lambda_h = 5.6(2) \mu\text{s}^{-1}$  for the hf transition rate, a value that is considerably more accurate than previous measurements. Results are also reported for Na, Al, P, Cl, and K.

DOI: 10.1103/PhysRevA.64.042505

PACS number(s): 36.10.Gv, 25.30.-c

### I. INTRODUCTION

There is still much uncertainty about the hyperfine transition rate for muonic atoms in the  $1s$  ground state. Different techniques often give different rates, and there are many inconsistencies. This topic was boosted into prominence 30 years ago by Winston and co-workers [1,2], who studied  $^{19}\text{F}$  and established the major properties of this effect. Even today,  $^{19}\text{F}$  remains the best understood example, because of the convenient time constant of about 180 ns.

When a  $\mu^-$  stops in a target, it forms a muonic atom, and quickly cascades down to the  $1s$  level on a time scale of  $10^{-12}$  s, which is effectively instantaneous for any detector. If the nucleus has no spin, there is a single ground state and the muon awaits its fate via the weak interaction decay ( $\mu^- \rightarrow e^- \bar{\nu}_e \nu_\mu$ ) or via nuclear capture. For the light elements this occurs within a few microseconds and can be studied with a variety of detectors. If the nucleus has a non-zero spin, however, the situation is more complicated because there are two hyperfine levels of the  $1s$  state, separated by an energy varying between a few eV and a keV or so. If the transition between these levels occurs via an  $M1$  photon, the rate is too slow to be observed. However, Winston & co-workers showed that Auger emission can speed up the transition rate a thousandfold and bring it to the time scale of nanoseconds, which is within the range of standard detectors. The hyperfine transition can be detected in any nucleus by observing the depolarization of the  $\mu^-$  via the detection of its decay electron. However, the  $\mu^-$  has a very small residual polarization in the atomic state ( $<10\%$  for nuclei with spin), and in addition the  $\mu^-$  can be depolarized by magnetic

interactions or by nearby radicals. Nevertheless, several experiments have been carried out successfully.

If the nucleus has an odd  $Z$ , the  $\mu^-$  is magnetically coupled to the odd proton. Now the capture probability in the  $\mu^-p$  system is  $660 \text{ s}^{-1}$  for the singlet state, but only  $12 \text{ s}^{-1}$  for the triplet state. Thus, assuming half of the protons are spin aligned with the muon, and the other half are antialigned, in one hyperfine state the total muon capture probability is approximately proportional to  $(Z+1)/2$  and in the other proportional to  $(Z-1)/2$ . Thus nuclear capture is quite sensitive to the hyperfine state, and the hyperfine transition can be followed by detecting neutrons from the capture events. The effect can also be observed via the time dependence of the decay electron, but in light nuclei the normal decay rate dominates and thus dilutes the signal. Winston [2] as well as Suzuki *et al.* [3] were able to observe this effect in  $^{19}\text{F}$ , but for other nuclei the signal is too small.

The hyperfine transition can also be observed by detecting specific  $\gamma$  rays resulting from nuclear capture. Some transitions are highly sensitive to the initial hyperfine state and, for certain spin combinations, this is also true for even- $Z$  nuclei such as  $^{13}\text{C}$ . Several nuclei have been studied by Gorringer and co-workers [4–7]. In addition Wiaux [8] has found a very large sensitivity for the 320 keV  $\gamma$  ray from muon capture in  $^{11}\text{B}$ . An unexpected observation by Gorringer *et al.* was that the hyperfine rate in metallic sodium was  $\Lambda_h = 15.5 \pm 1.1 \mu\text{s}^{-1}$  [5], but in NaF the sodium hyperfine rate was only  $\Lambda_h = 8.4 \pm 1.9 \mu\text{s}^{-1}$  [4]; the fluorine hyperfine rate was  $\Lambda_h = 4.9 \pm 1.2 \mu\text{s}^{-1}$ , consistent with Winston's measurement of  $\Lambda_h = 6.1 \pm 0.7 \mu\text{s}^{-1}$  [2], and our own measurement of  $\Lambda_h = 5.6 \pm 0.2 \mu\text{s}^{-1}$  in LiF. This raised the possibility that there might be a difference between metals and insulators, or between different molecular species. Such a difference could be due to different times for the electrons, ejected during the muonic cascade, to return to the muonic atom and recombine, or due to an unusual sensitivity to the binding energy of the valence electrons. Remember that the hyperfine transition proceeds via the Auger emission of weakly bound electrons. Both possibilities seem unlikely, however.

The most puzzling result to date has been the observation of a hyperfine transition in  $^{14}\text{N}$  by Ishida *et al.* [9], using the muon spin resonance ( $\mu^-$ -SR) technique to observe the muon depolarization. In this technique a polarized  $\mu^-$  is

\*Present address: Communications Research Centre, 3701 Carling Avenue, Box 11490, Station H, Ottawa, Ontario, Canada K2H 8S2. Email address: trevor.stocki@crc.ca

<sup>†</sup>Present address: London Regional Cancer Centre, 790 Commissioner Road East, London, Ontario, Canada N6A 4L6.

<sup>‡</sup>Present address: Faculty of Engineering, University of Malta, Msida MSD 06, Malta.

<sup>§</sup>Present address: Defense Research Establishment Ottawa, 3701 Carling Avenue, Ottawa, Ontario, Canada K1A 0Z4.

stopped in an atom in a magnetic field and the spin precession is detected via the parity violating asymmetry of the decay electrons. If there is a hyperfine transition, the electron asymmetry decreases accordingly. Unfortunately, the residual polarization of the  $\mu^-$  is only about 10% for a nucleus with spin, so experiments are quite difficult. Now, for nitrogen, Ishida *et al.* observed a relaxation rate of  $0.092(33) \mu\text{s}^{-1}$  of which about  $0.016 \mu\text{s}^{-1}$  is due to the different loss rates from the hyperfine states. This leaves  $0.076(33) \mu\text{s}^{-1}$  that may be from a hyperfine transition. The problem is that the energy difference between the hyperfine states is only 7.4 eV, whereas, in the carbon atom, the least bound electron is bound by 11.3 eV, i.e., this energy is the ionization potential (the  $\mu^-$  is close to the nucleus, so the  $^{14}\text{N}$  muonic system appears to the electrons to be more like a  $^{14}\text{C}$  nucleus). If the pseudo  $^{14}\text{C}$  atom has formed a “C” N bond, the ionization potential is 14.3 eV, which makes the matter worse. We note that Wiaux found a slower hyperfine rate in  $^{11}\text{B}$  in comparison to a  $\mu\text{SR}$  experiment, so we suggest that the observation in  $^{14}\text{N}$  was caused by an additional depolarization mechanism, not the hyperfine transition.

Because of the various inconsistencies in this field, it was decided to reinvestigate several light nuclei, using the more reliable technique of neutron detection. A comparison was also desirable between Na and NaH, Al and  $\text{LiAlH}_4$ , and K and KH, to see if any difference could be detected. Unfortunately, no satisfactory result was obtained for KH. It should be noted that any muon captured in hydrogen is immediately transferred to another atom with higher  $Z$ , because the  $\mu p$  system is neutral. Thus NaH, for example, is effectively pure sodium in an insulating environment.

## II. EXPERIMENTAL TECHNIQUE

The experiment was carried out in the M9B channel at TRIUMF, which includes a superconducting solenoid. For muons of 60 MeV/ $c$  the stop rate was  $\approx 10^4 \text{ s}^{-1}$  with an electron contamination of 20% and a pion contamination of  $\leq 0.2\%$ . The muons passed through two plastic scintillators, and stopped in various targets; a third large plastic scintillator was used as a veto to define a muon stopped in the target. Almost all the beam stopped in the target. Empty target runs indicated that 1.8% of the muons stopped in the scintillators when no degrader was used and 4.5% when a degrader was used. However, only 7.8% of muons are captured in carbon, to be compared with 33% in fluorine; thus in the worst case this background is divided by  $\approx 4$ . A  $\mu$ -metal shield around the targets reduced the ambient magnetic field from 1.5 to 0.1 G. Table I lists the properties of the targets. The elemental sodium target was cut clean, and stored under  $\text{N}_2$  in a plastic target container, which had a rubber o-ring seal.

The neutron detectors were four cylindrical liquid scintillators, two of NE213, one of NE224, and one of BC501A (equivalent to NE213). They were arranged in a symmetrical array at  $45^\circ$ ,  $135^\circ$ ,  $225^\circ$ , and  $315^\circ$  to the beam, in order to minimize muon spin rotation effects. Plastic scintillators were placed in front of each detector to veto charged particles (such as decay electrons). The counters had a timing resolution of better than 5 ns full width at half maximum for

TABLE I. Properties of the targets used.

$Z$	Target	Thickness ( $\text{g}/\text{cm}^2$ )	Number of events in time spectrum
3,9	LiF	2.70	$1.2 \times 10^6$
6,9	$(\text{CF}_2)_n$	2.25	$3.5 \times 10^5$
11	NaH	1.14	$1.5 \times 10^6$
11	Na	1.65	$1.5 \times 10^6$
12	Mg	1.61	$2.2 \times 10^5$
13	Al	4.69	$1.2 \times 10^6$
13	$\text{LiAlH}_4$	1.51	$1.9 \times 10^5$
14	Si	3.55	$3.0 \times 10^5$
15	P	2.79	$2.8 \times 10^6$
17	LiCl	2.60	$7.6 \times 10^5$
17	$\text{CCl}_4$	6.18	$4.9 \times 10^5$
19	K	1.78	$8.4 \times 10^5$
29,30	Brass (Cu+Zn)	2.79	$1.8 \times 10^5$
79	Au	1.83	$2.7 \times 10^5$

$\gamma$  rays. The counters were 34.6 cm from the target so the  $\gamma$ -ray time of flight is 1.15 ns.

Pulse shape discrimination was used to distinguish neutrons from  $\gamma$  rays. Two different modules were used at different times, but the discrimination was always set conservatively [10]. Sources of  $^{60}\text{Co}$  and AmBe were used to set up the system. If  $\gamma$  rays are detected during the experiment, a prompt peak is clearly distinguishable, so it is straightforward to monitor the electronics on line.

The time of arrival of an event with respect to the stopping muon was measured by both a 5  $\mu\text{s}$  and a 10  $\mu\text{s}$  full scale time to digital converter (TDC). These TDCs have been tested and do not contribute significantly to the errors in the experiment. The data were stored with a binning width of 2.517 ns, but were rebinned for figures.

Data acquisition was carried out by a VAX station 3200 and a PDP-11 front-end processor (starburst). Data collected from the computer automated measurement and control

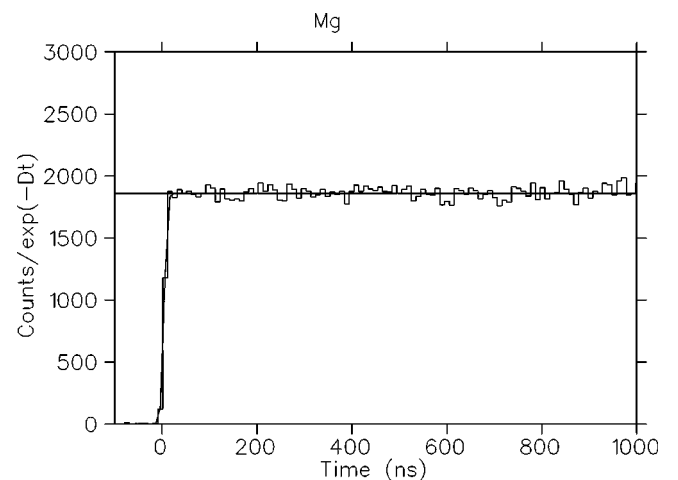


FIG. 1. The time spectrum of neutrons from muon capture in Mg, fitted to Eq. (1). The data are presented with the muon disappearance rate divided out.

TABLE II. Values of  $S$  and  $t_0$  from nonhyperfine targets. Also given are the average energy  $\bar{E}$  and the energy spread  $\Delta E$  of the neutron events used for the timing measurements.

$Z$	Target	$S$ (ns)	$t_0$ (ns)	$\Delta t$ (ns)	$\bar{E}$ (MeV)	$\Delta E$ (MeV)
12	Mg	$4.63 \pm 0.24$	$4.22 \pm 0.23$	$5.37 \pm 0.23$	$22.4 \pm 2.1$	$34 \pm 12$
14	Si	$5.26 \pm 0.17$	$5.14 \pm 0.17$	$6.29 \pm 0.17$	$16.2 \pm 0.9$	$25 \pm 8$
16	S	$4.84 \pm 0.12$	$4.35 \pm 0.14$	$5.50 \pm 0.14$	$21.4 \pm 1.2$	$29 \pm 9$
29,30	Brass (Cu+Zn)	$5.92 \pm 0.11$	$9.72 \pm 0.11$	$10.87 \pm 0.11$	$5.3 \pm 0.1$	$19 \pm 5$
79	Au	$6.93 \pm 0.08$	$13.36 \pm 0.07$	$14.51 \pm 0.07$	$2.98 \pm 0.03$	$14 \pm 3$

(CAMAC) modules were written to 8 mm tapes for later analysis. Further technical details of the equipment are available in the thesis by Stocki [10].

To test the overall system several targets were chosen for which there is no hyperfine transition, or for which the transition is too fast to be observed. The time of arrival of the neutrons could then be fitted by the formula

$$N(t) = \left( \frac{1}{2} \operatorname{erf} \frac{t-t_0}{\sqrt{2}S} + \frac{1}{2} \right) C e^{-Dt} + B, \quad (1)$$

where erf stands for the error function,  $D$  is the total disappearance rate for the element under study,  $B$  is a flat background,  $t_0$  is the midpoint of the rise-time curve, and  $S$  is a folding of the time of flight spread and instrumental time resolution (i.e., this assumes a Gaussian time distribution with a standard deviation of  $S$  for the combination of these effects).

A typical fit for Mg is illustrated in Fig. 1. The values for  $S$  and  $t_0$  are presented in Table II and show the tendency for heavier elements to have a slower time of flight for the neutrons. As  $t$  is calibrated to be zero for the time of arrival of the  $\gamma$  rays, one can add the  $\gamma$ -ray time of flight (1.15 ns) to obtain the average neutron time of flight ( $\Delta t$ ) and average neutron energy ( $\bar{E}$ ). From  $S$  one can remove the counter timing resolution to obtain the spread in energy of the neutrons ( $\Delta E$ ). These values were used as guidance in analyzing the elements with a hyperfine effect. Note that these values for  $\bar{E}$  and  $\Delta E$  are for the neutrons detected in this experiment, and do not constitute measurements of these parameters for muon capture in general.

By taking the time derivative of the data such as that shown in Fig. 1, one can get an idea of the neutron time of flight and detector resolution effects. Figure 2 shows these time derivative spectra for Au, brass, Si, and S. One can clearly see in brass and Au that a single error function (or Gaussian) is not enough. We found that the function

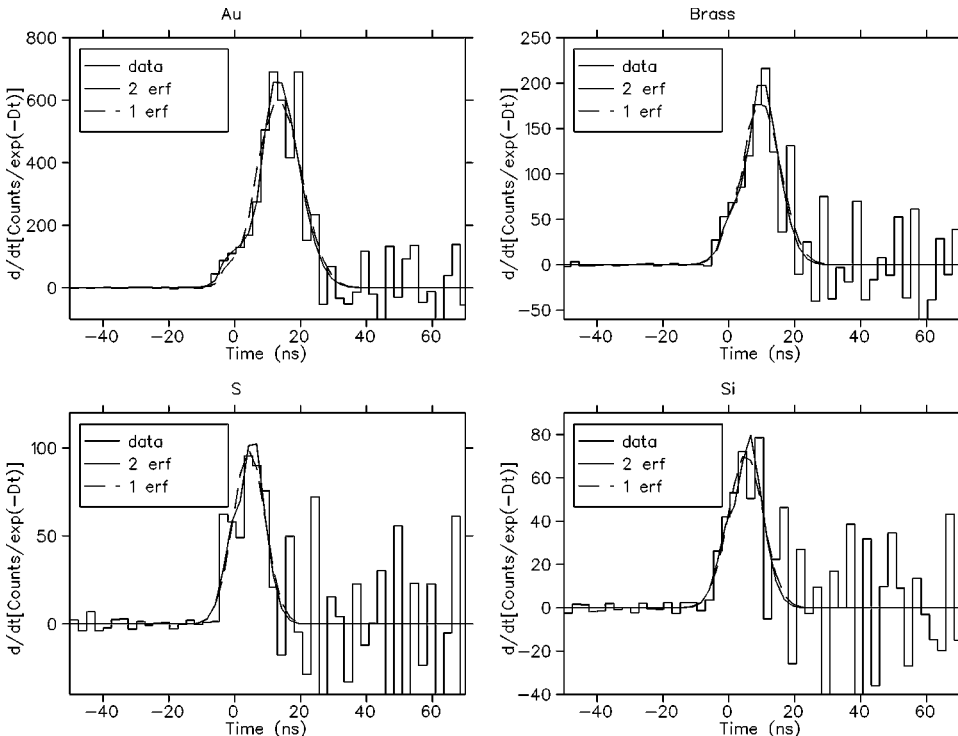


FIG. 2. The time derivative spectra of neutrons from muon capture in Au, brass, Si, and S fitted to Eq. (1) and Eq. (2). The time derivative was taken of both the fit and the data after the fit was done.

$$N(t) = \left[ \frac{1}{2} \operatorname{erf} \frac{t-t_0}{\sqrt{2}S} + \frac{1}{2} + R \left( \frac{1}{2} \operatorname{erf} \frac{t-t_1}{\sqrt{2}S_1} + \frac{1}{2} \right) \right] C e^{-Dt} + B \quad (2)$$

seems to give a better fit to the data for those elements (i.e., the original data, not the time derivative). The effect is not seen in Si and S, due to limited statistics.

For most elements there was a small correction (a few percent) for background from muons stopping in carbon in the scintillators. In addition, a few targets contained two elements, viz., LiF,  $(\text{CF}_2)_n$ , LiCl, and  $\text{CCl}_4$ . We used Teflon, i.e.,  $(\text{CF}_2)_n$ , and  $\text{CCl}_4$  as test cases to ensure that the corrections could be adequately applied. For such molecular targets one needs to know the atomic capture ratio. The Fermi-Teller  $Z$  law is far from adequate and a  $Z^{1/3}$  variation gives a better approximation [11]. However, it is far more satisfactory to use an actual measurement as the empirical variation is significant.

For LiF the atomic capture ratio (Li/F) has been measured to be 0.28(3) by Zinov *et al.* [12] and 0.10(8) by Wilhelm *et al.* [13] for muons, and 0.10(1) [14] and 0.22(2) [15] for pions, which should be the same. As Zinov *et al.*'s results disagree with later measurements for several other molecules, we take the pion values and use 0.16(12) with a liberal error. This value agrees with the empirical capture probability for muons determined by von Egidy and Hartmann, which is 0.18(5) for LiF [16]. For  $(\text{CF}_2)_n$ , Martoff *et al.* [15]

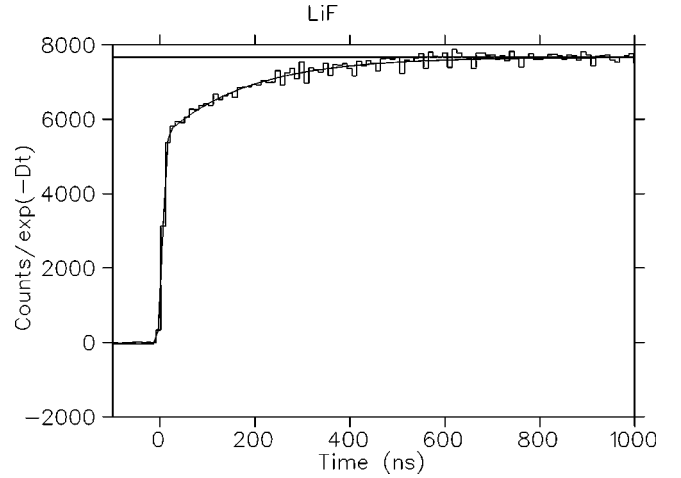


FIG. 3. The time spectrum of LiF, with the decay divided out. The hyperfine transition in fluorine is clearly visible with its time constant of about 180 ns.

found that  $(89.4 \pm 0.7)\%$  of pions capture on fluorine, i.e., an atomic capture ratio C/F of 0.24(2) in the normal definition, which takes into account the relative number of atoms. The  $Z^{1/3}$  law gives 0.87; von Egidy and Hartmann [16] do not give a value for carbon, but using the Martoff value, and a measurement of  $\text{CO}_2$  [17], we estimate that the C capture probability is 0.33(9) in the von Egidy-Hartmann scheme. We note that this C:O ratio can vary between 0.5 and 0.8 in

TABLE III. Values of  $S$  and  $t_0$  for hyperfine targets, and their effect on the systematic uncertainties of  $H$  and  $A$ . One row for two error functions uses a shape derived from the brass data, the other row uses the shape of the gold data. The different results for  $H$  and  $A$  for each target should be taken as a measure of the systematic uncertainties.

$Z$	Target	$S$ (ns)	$t_0$ (ns)	Type of error function	$H$ ( $\mu\text{s}^{-1}$ )	$A$ (unitless)
9	LiF	$5.38 \pm 0.18$	$5.30 \pm 0.17$	1	$5.6 \pm 0.2$	$0.288 \pm 0.006$
		$4.92 \pm 0.15$	$4.81 \pm 0.15$	2	$5.7 \pm 0.3$	$0.290 \pm 0.006$
		$5.31 \pm 0.20$	$5.87 \pm 0.18$	2	$5.6 \pm 0.2$	$0.287 \pm 0.006$
9	$(\text{CF}_2)_n$	$5.03 \pm 0.31$	$5.18 \pm 0.29$	1	$5.2 \pm 0.4$	$0.33 \pm 0.01$
		$4.68 \pm 0.26$	$4.59 \pm 0.27$	2	$5.2 \pm 0.4$	$0.33 \pm 0.01$
		$4.89 \pm 0.36$	$5.71 \pm 0.31$	2	$5.2 \pm 0.4$	$0.33 \pm 0.01$
11	NaH	$5.0 \pm 0.2$	$5.0 \pm 0.1$	1	$26 \pm 4$	$0.15 \pm 0.02$
		$4.31 \pm 0.22$	$4.51 \pm 0.13$	2	$32 \pm 4$	$0.19 \pm 0.03$
		$4.94 \pm 0.16$	$5.54 \pm 0.22$	2	$26 \pm 5$	$0.15 \pm 0.02$
11	Na	$4.7 \pm 0.1$	$4.5 \pm 0.2$	1	$39 \pm 7$	$0.18 \pm 0.04$
		$4.23 \pm 0.13$	$3.77 \pm 0.32$	2	$49 \pm 10$	$0.24 \pm 0.06$
		$5.21 \pm 0.23$	$4.75 \pm 0.14$	2	$34 \pm 6$	$0.15 \pm 0.03$
13	Al	$5.13 \pm 0.13$	$3.52 \pm 0.38$	1	$68 \pm 9$	$0.30 \pm 0.06$
		$4.63 \pm 0.13$	$2.73 \pm 0.30$	2	$75 \pm 7$	$0.37 \pm 0.04$
		$5.21 \pm 0.23$	$4.75 \pm 0.14$	2	$71 \pm 9$	$0.31 \pm 0.06$
13	$\text{LiAlH}_4$	$5.04 \pm 0.31$	$2.37 \pm 0.45$	1	$90 \pm 6$	$0.50 \pm 0.04$
		$4.96 \pm 0.23$	$4.66 \pm 0.85$	2	$53 \pm 25$	$0.22 \pm 0.13$
15	P	$6.51 \pm 0.07$	$5.7 \pm 0.23$	1	$44 \pm 8$	$0.12 \pm 0.03$
		$5.90 \pm 0.07$	$4.57 \pm 0.19$	2	$62 \pm 6$	$0.23 \pm 0.03$
		$6.73 \pm 0.11$	$5.45 \pm 0.20$	2	$76 \pm 5$	$0.27 \pm 0.02$

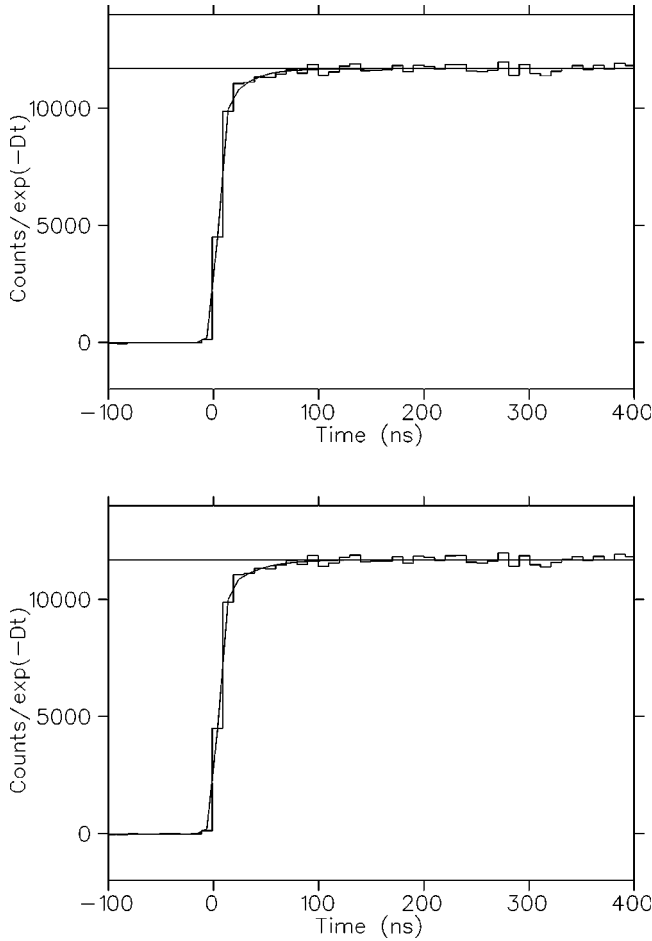


FIG. 4. The time spectrum of Na, with the decay divided out for the one-error-function case (top) and the two-error-function case (bottom).

various organic molecules, but we believe that the data on  $\text{CF}_2$  and  $\text{CO}_2$  are more relevant for  $\text{CCl}_4$ . For  $\text{CCl}_4$  there is no measurement but using our value of the C capture probability we obtain  $\text{C}/\text{Cl} = 0.25(7)$ , i.e.,  $(5.8 \pm 1.6)\%$  of muons stop in the carbon of  $\text{CCl}_4$ . The  $Z^{1/3}$  rule gives  $\text{C}/\text{Cl} = 0.71$ , i.e., 15% of muons stop in the carbon of  $\text{CCl}_4$ . For  $\text{LiCl}$  the atomic capture ratio as measured by Daniel *et al.* [18] is 0.19(8).

Although these values are very uncertain, the situation is not as bad as it might appear. For the lighter elements there are many fewer neutrons produced per muon stop, so the corrections turn out to be fairly minor. For example, the number of stops in an element for which capture occurs (most of which produce neutrons) are 0.53% for Li, 7.8% for C, 33% for F, and 75% for Cl [3]. The effective background, therefore, from lithium in  $\text{LiF}$  is 0.25%, which is negligible in comparison to other problems. We assume the neutron multiplicity to be the same for all these elements.

### III. EXPERIMENTAL RESULTS

The results for elements with a hyperfine effect are fitted to two different functions; one with a single error function, viz.,

TABLE IV. Muonic hyperfine transition rates in  $\mu\text{s}^{-1}$ . Our values are a weighted average of all fits listed in Table III.

Compound	Theory [2]	Previous work	This experiment
LiF	5.8	$5.8 \pm 0.8$ [2] $6.3 \pm 1.8$ [2]	$5.6 \pm 0.2$
NaF		$4.9 \pm 1.2$ [4]	$5.2 \pm 0.4$
$(\text{CF}_2)_n$			
Na	14	$15.5 \pm 1.1$ [5]	$38 \pm 9$
NaH			$28 \pm 5$
NaF		$8.4 \pm 1.9$ [4]	
Al	41	$41 \pm 9$ [23]	$72 \pm 9$
$\text{LiAlH}_4$			$88 \pm 10$
Red P	58	$\lambda_h \gg \lambda_-^a$ [4] $\lambda_- \gg \lambda_h$ [22]	$65 \pm 15$
LiCl	8	$6.5 \pm 0.9$ [4]	$14 \pm 27$
$\text{CCl}_4$			$15 \pm 29$
K	22		$25 \pm 15$

<sup>a</sup> $\lambda_- \approx 1.1 \mu\text{s}^{-1}$ .

$$N(t) = \left[ \text{erf} \frac{t-t_0}{\sqrt{2S}} + 1 \right] [C e^{-Dt} (1 - A e^{-Ht}) + F e^{-Gt} + P e^{-Qt}] + B, \quad (3)$$

and another more complex version with two error functions:

$$N(t) = \left[ \frac{1}{2} \text{erf} \frac{t-t_0}{\sqrt{2S}} + \frac{1}{2} + R \left( \frac{1}{2} \text{erf} \frac{t-t_1}{\sqrt{2S_1}} + \frac{1}{2} \right) \right] \times [C e^{-Dt} (1 - A e^{-Ht}) + F e^{-Gt} + P e^{-Qt}] + B \quad (4)$$

where  $H$  is the hyperfine rate,  $A$  is the hyperfine asymmetry,  $F$  and  $G$  are contributions from carbon in the counters,  $P$  and  $Q$  are contributions from other elements (if appropriate), and  $B$  is a flat background. This function for the hyperfine transition was derived by Winston [2,19]. The parameters  $F$ ,  $G$ ,  $P$ , and  $Q$  were calculated and fixed. We have also used an overall value for  $t_0$ ,  $S$ , and  $S_1$  because these background components make no substantial contribution to the data analysis. By using these two equations we can get a handle on the systematic errors. In Eq. (4) we tie the  $S_1$  and  $t_1$  values to the  $S$  and  $t_0$  for two cases, using fits to the brass and the Au data. For  $\text{LiF}$  the data were of sufficient quality that all the other parameters ( $t_0, S, C, D, A, H$ ) could be fitted freely. In this case the hyperfine effect is well separated from the rise-time effect caused by the neutron time of flight effects. The best fit for fluorine is illustrated in Fig. 3 and the values of  $S$  and  $t_0$  for all hyperfine targets are given in Table III. They are consistent with the nonhyperfine elements but slightly different. For the two error function fits, one row uses the  $R$ ,  $S_1$ , and  $t_1$  found for the brass data, and the other row uses the values from the gold data. These were fixed and the difference indicates the effect of this shape difference. Note that  $t_0$  is no longer simply related to the average time of flight (and the average neutron energy).

TABLE V. The capture rate asymmetry. The theory values are for all captures. This experiment is for neutron detection only (weighted by multiplicity). BLYP (Bernstein, Lee, Yang, and Primakoff) and Primakoff are theoretical estimates, quoted by Winston [2].

Compound	BLYP [2]	Primakoff [2]	Überall [24]	Previous work [2]	This experiment
LiF	0.24	0.36	0.36	$0.36 \pm 0.04(n)$ $0.25 \pm 0.04(\gamma)$ $0.29 \pm 0.02(n\gamma)$	$0.29 \pm 0.01$
$(CF_2)_n$	0.24	0.36	0.36		$0.33 \pm 0.01$
Na	0.08				$0.17 \pm 0.05$
NaH	0.08				$0.16 \pm 0.03$
Al	0.09	0.14	0.22		$0.34 \pm 0.05$
LiAlH <sub>4</sub>	0.09	0.14	0.22		$0.35 \pm 0.15$
Red P	0.16	0.22	0.25		$0.2 \pm 0.1$
LiCl	$-0.06(^{35}\text{Cl})$ $-0.06(^{37}\text{Cl})$	$-0.10(^{37}\text{Cl})$			$-0.03 \pm 0.06$
CCl <sub>4</sub>					$-0.03 \pm 0.06$
K	-0.05	-0.07			$-0.080 \pm 0.055$

The different fits constitute a salutary warning and we shall need to use both Eqs. (3) and (4) to get a handle on the systematic errors due to the time of flight and timing resolution effects. Our recommended values are the averages of these two methods. One would think that one could get the values of  $S$  and  $t_0$  from the time spectra of the neighboring  $0^+$  nuclei. This turns out to be a bad assumption. First let us understand the physics behind this hypothesis. Nuclei without a hyperfine effect are  $0^+$  nuclei, often even-even nuclei such as  $^{16}\text{O}$ ,  $^{24}\text{Mg}$ ,  $^{28}\text{Si}$ , and  $^{40}\text{Ca}$ . These are tightly bound. However, odd- $Z$  nuclei like  $^{19}\text{F}$ ,  $^{23}\text{Na}$ ,  $^{27}\text{Al}$ , and  $^{31}\text{P}$  tend to have  $N=Z+1$  and so transforming a proton to a neutron proceeds to a nucleus even more neutron rich and more likely to fall apart. The typical neutron energy spectrum after muon capture is composed of two components, an evaporation spectrum peaked at about 1.5 MeV followed by a high energy tail starting around 5 or 6 MeV [20]. Setting a threshold at 10 MeV, Kozłowski *et al.* [21] have shown that high energy neutrons constitute the following fraction: 26(5)% in  $^{16}\text{O}$ , 19(3)% in  $^{28}\text{Si}$ , 11(2)% in Ca, and 11(2)% in Pb. Thus for light elements the high energy component is very important, and it is not surprising if it is sensitive to details of the nuclear structure of the product nucleus. The results of our experiment confirm that there are significant variations from nucleus to nucleus.

For Na, Al, P, Cl, and K we do not have sufficient data to allow a free parameter search, so we must average the single-error-function results with the two-error-function results, otherwise we do not know whether the results are from both time of flight and hyperfine effects. Notice that for LiF and  $(CF_2)_n$  this does not have to be done, because in F the capture rate asymmetry is large enough and the hyperfine rate is slow enough that the hyperfine rate can be distinguished from the time of flight effects. One way out of the dilemma for the other elements is to raise the energy threshold on the neutron detector. However, the hyperfine asymmetries are very small, and statistics becomes a problem. The other way is to do a full study of the neutron spectrum but this is a

major project. We have therefore been forced to simply compare results from different fitting functions, using shape information from the spectra in Fig. 2. The difference between the fits gives us an estimate of the systematic error. Figure 4 shows two fits for Na which are both quite satisfactory and very hard to distinguish by eye. In Table IV our final recommended values are compared with previous results and the hyperfine asymmetries are compared in Table V to various theories and previous experiments. Note that in Table IV the Cl and K results did not use these error functions; since their asymmetry values were less than 0, the hyperfine effect could be easily distinguished from the neutron time of flight effects. The most important feature is that, apart from  $^{19}\text{F}$  and to some extent  $^{23}\text{Na}$ , the hyperfine asymmetries are small, and that creates part of the problem. The  $\gamma$ -ray experiments observe large asymmetries (and  $\gamma$  rays all travel at the same speed). Thus  $\gamma$ -ray experiments with lower statistics can effectively compete with neutron-detection experiments. A word of caution should be given concerning the comparison of the asymmetry with previous calculations, which were made for the total capture rates (including transitions to bound levels that give off no neutrons and to levels that give off two neutrons). The experimental asymmetries are for specific experimental conditions with a threshold on the neutron energy and an energy dependent efficiency for the neutron detector. Thus one would not expect an exact equivalence, but the comparison is interesting.

We see that, on the whole, the errors on the hyperfine rate are somewhat large. The two results that are most convincing are F and Na, but the latter is not sufficient to resolve the disagreement between the earlier sodium metal and NaF results.

The phosphorus result is worth a short discussion. An initial polarization measurement by Egorov *et al.* [22] claimed that an asymmetry had been observed. The measurement was from 0 to 2.4  $\mu\text{s}$  implying no fast depolarization. Note also that the upper level is  $F=1$  and the lower level  $F=0$ , so that if a fast hyperfine transition does occur there

can be no residual polarization. Later asymmetry measurements by Hutchinson *et al.* [25] and Babaev *et al.* [26] observed no asymmetry and set limits at 10% of the value observed by Egorov *et al.*, thus indicating that the hyperfine transition was fast, as suggested by Winston [2], who calculated  $58 \mu\text{s}^{-1}$ , i.e.,  $\tau=17$  ns. This scenario is consistent with the data of Gorringer *et al.* [5] using  $\gamma$ -ray detection, but no positive observation was obtained. Again, our own result has systematic difficulties but is a positive identification of the hyperfine transition in phosphorus. All the other hyperfine rates are consistent with earlier results.

The comparison of Na and NaH in our data is interesting, but not of sufficient quality to resolve the questions about the sodium hyperfine rate in metal and in NaF; similarly for Al and  $\text{LiAlH}_4$ , though the trend is for the hyperfine rates to be similar.

In conclusion, we have measured the hyperfine rate in P and obtained a more accurate value for F. Even though neutron detection appears to be the most sensitive technique for measuring the hyperfine transition rate, the problems with the neutron energy spectrum and the spread of the time of flight to the detectors have made it very difficult to observe

fast rates. Further experiments should use a higher energy threshold (and take considerably greater statistics). An alternative technique would be to use a  $\gamma$ -ray detector with a high resolution, but a faster time response than a high purity Ge detector. Such detectors are now being developed.

#### ACKNOWLEDGMENTS

We wish to thank Glen Marshall and Elie Korkmaz for lending some liquid scintillators and some pulse shape discriminator Nuclear Instrument Module (NIM) units to us. We would also like to thank B. A. Moftah and M. C. Fujiwara for their help and advice with the experiment. We thank Lars Holm for his help with the University of Alberta pulse shape discrimination NIM module. We wish to thank the Natural Sciences and Engineering Research Council of Canada and similarly the National Science Foundation in the U.S.A. for providing support and equipment for this experiment; we also thank the National Research Council of Canada and the staff at TRIUMF for providing the excellent muon beam facility.

- 
- [1] G. Gulligan, J.F. Lathrop, V.L. Telegdi, R. Winston, and R.A. Lundy, *Phys. Rev. Lett.* **7**, 458 (1961).
  - [2] R. Winston, *Phys. Rev.* **129**, 2766 (1963).
  - [3] T. Suzuki, D.F. Measday, and J.P. Roalsvig, *Phys. Rev. C* **35**, 2212 (1987).
  - [4] T.P. Gorringer *et al.*, *Phys. Lett. B* **309**, 241 (1993).
  - [5] T.P. Gorringer *et al.*, *Phys. Rev. Lett.* **72**, 3472 (1994).
  - [6] B. Johnson *et al.*, *Phys. Rev. C* **54**, 2714 (1996).
  - [7] T.P. Gorringer *et al.*, *Phys. Rev. C* **60**, 055501 (1999).
  - [8] V. Wiaux, Ph.D. thesis, Université catholique de Louvain, 1999.
  - [9] K. Ishida *et al.*, *Phys. Lett.* **167B**, 31 (1986).
  - [10] T.J. Stocki, Ph.D. thesis, University of British Columbia, 1999.
  - [11] D. Horvath and F. Entezami, TRIUMF Report No. TRI-83-1 (unpublished).
  - [12] V.G. Zinov *et al.*, *Sov. J. Nucl. Phys.* **2**, 613 (1966).
  - [13] W. Wilhelm *et al.*, *Chem. Phys. Lett.* **55**, 478 (1978); see also F.J. Hartmann *et al.*, *Z. Phys. A* **308**, 103 (1982).
  - [14] N. Imanishi *et al.*, *Phys. Rev. A* **37**, 43 (1988).
  - [15] C.J. Martoff *et al.*, *Phys. Rev. C* **27**, 1621 (1983).
  - [16] T. von Egidy and F.J. Hartmann, *Phys. Rev. A* **26**, 2355 (1982).
  - [17] T. Suzuki *et al.*, *Phys. Lett.* **95B**, 202 (1980).
  - [18] H. Daniel *et al.*, *Z. Phys. A* **300**, 253 (1981).
  - [19] R. Winston and V.L. Telegdi, *Phys. Rev. Lett.* **7**, 104 (1961).
  - [20] W.U. Schröder *et al.*, *Z. Phys.* **268**, 57 (1974).
  - [21] T. Kozłowski *et al.*, *Nucl. Phys. A* **436**, 717 (1985).
  - [22] L.B. Egorov *et al.*, *Sov. Phys. JETP* **14**, 494 (1962); I.E. Ignatenko *et al.*, *Nucl. Phys.* **32**, 563 (1962).
  - [23] J.H. Brewer, *Hyperfine Interact.* **17–19**, 879 (1984).
  - [24] H. Überall, *Phys. Rev.* **121**, 1219 (1961).
  - [25] D.P. Hutchinson *et al.*, *Phys. Rev. Lett.* **9**, 516 (1962).
  - [26] A.I. Babaev *et al.*, *Sov. J. Nucl. Phys.* **10**, 554 (1970).